

## SHORT COMMUNICATION

# Frequent side chain methyl carbon-oxygen hydrogen bonding in proteins revealed by computational and stereochemical analysis of neutron structures

Joseph D. Yesselman,<sup>1,2</sup> Scott Horowitz,<sup>1,3,4\*</sup> Charles L. Brooks III,<sup>1,5</sup> and Raymond C. Trievel<sup>4\*</sup>

<sup>1</sup> Department of Biophysics, University of Michigan, Ann Arbor, Michigan 48109

<sup>2</sup> Department of Biochemistry, Stanford University, Stanford, California 94305

<sup>3</sup> Department of Molecular, Cellular, and Developmental Biology, University of Michigan, Ann Arbor, Michigan 48109

<sup>4</sup> Department of Biological Chemistry, University of Michigan, Ann Arbor, Michigan 48109

<sup>5</sup> Department of Chemistry, University of Michigan, Ann Arbor, Michigan 48109

### ABSTRACT

The propensity of backbone C $\alpha$  atoms to engage in carbon-oxygen (CH $\cdots$ O) hydrogen bonding is well-appreciated in protein structure, but side chain CH $\cdots$ O hydrogen bonding remains largely uncharacterized. The extent to which side chain methyl groups in proteins participate in CH $\cdots$ O hydrogen bonding is examined through a survey of neutron crystal structures, quantum chemistry calculations, and molecular dynamics simulations. Using these approaches, methyl groups were observed to form stabilizing CH $\cdots$ O hydrogen bonds within protein structure that are maintained through protein dynamics and participate in correlated motion. Collectively, these findings illustrate that side chain methyl CH $\cdots$ O hydrogen bonding contributes to the energetics of protein structure and folding.

Proteins 2015; 83:403–410.  
© 2014 Wiley Periodicals, Inc.

**Key words:** CH $\cdots$ O; C–H $\cdots$ O; CH–O; CH $\cdots$ O C–H $\cdots$ O; hydrogen bond; neutron structure; molecular dynamics; quantum mechanics.

### INTRODUCTION

CH $\cdots$ O hydrogen bonds are well-recognized interactions<sup>1</sup> in protein structure, particularly those formed by backbone C $\alpha$  atoms. These hydrogen bonds are energetically stabilizing,<sup>1</sup> and play roles in diverse biological processes, from protein structure and folding to signal transduction and enzyme catalysis.<sup>2</sup> Recently, the highly polarized methyl group of S-adenosylmethionine (AdoMet) has been shown to form strong CH $\cdots$ O hydrogen bonds within the active sites of AdoMet-dependent methyltransferases.<sup>3</sup> However, the

Additional Supporting Information may be found in the online version of this article.

Grant sponsor: NSF grant; Grant number: CHE-1213484; Grant sponsor: NIH; Grant number: GM037554.

Joseph D. Yesselman and Scott Horowitz contributed equally to this work

\*Correspondence to: Raymond C. Trievel, University of Michigan, Ann Arbor, MI 48109. E-mail: rtrivel@umich.edu

Scott Horowitz current address is Howard Hughes Medical Institute, Ann Arbor, Michigan, 48109

Received 11 September 2014; Revised 19 October 2014; Accepted 10 November 2014

Published online 17 November 2014 in Wiley Online Library (wileyonlinelibrary.com). DOI: 10.1002/prot.24724

potential of side chain methyl groups, such as in alanine, threonine, methionine, leucine, isoleucine, and valine to participate in CH $\cdots$ O hydrogen bonding has not been investigated to date, as these groups are among the least polarized carbon atoms in proteins and are thus presumed not to engage in hydrogen bonding. Quantum mechanical (QM) calculations have demonstrated that methane, which is generally considered to be the least polarized of sp<sup>3</sup> carbon atoms, is capable of forming very weak CH $\cdots$ O hydrogen bonds, and that the strengths of CH $\cdots$ O hydrogen bonds correlates with the degree of polarization by the carbon donor due to covalently bonded heteroatoms.<sup>4,5</sup> Additionally, surveys of the Cambridge Structural Database demonstrated that in small molecules, aliphatic methyl groups are capable of engaging in CH $\cdots$ O hydrogen bonds as observed in neutron crystal structures,<sup>6,7</sup> while previous surveys of the PDB suggested that side chain methyl groups might similarly participate in hydrogen bonding in proteins.<sup>8,9</sup>

In our recent study characterizing CH $\cdots$ O hydrogen bonding between the AdoMet methyl group and the active sites of different methyltransferases,<sup>3</sup> we analyzed the potential formation of CH $\cdots$ O hydrogen bonds by side chain methyl groups as a control within this set of high-resolution crystal structures. Unexpectedly, nearly a third of the methyl groups in these proteins were classified as forming CH $\cdots$ O hydrogen bonds based on our distance and angular criteria, perhaps indicating that methyl groups are capable and willing to form hydrogen bonds in a protein environment. However, as this survey was performed on X-ray crystal structures, the position of the methyl hydrogen atoms were not experimentally defined, precluding conclusive determination of the extent of side chain methyl CH $\cdots$ O hydrogen bonding in these structures. These findings prompted us to more closely examine the extent and potential importance of side chain methyl CH $\cdots$ O hydrogen bonding in protein structure.

## MATERIAL AND METHODS

### Neutron structure survey

Neutron structures were chosen for CH $\cdots$ O bond analysis based on resolution and level of deuteration as previously described recently.<sup>10</sup> All perdeuterated neutron structures deposited in the PDB with modeled hydrogens were included, as well as all neutron structures solved to better than 2.0 Å resolution, excepting 4N3M, which noted distortions in hydrogen positions due to incoherent scattering. Our cutoffs choices were guided by a recent definition of hydrogen bonding<sup>11</sup> and van der Waals distances (See Supporting Information for discussion of van der Waals cutoffs). The distance cutoffs for methyl CH $\cdots$ O, CH $\cdots$ C, and OH $\cdots$ O hydrogen bonding were 2.7, 2.9, and 2.7 Å, respectively, based on the sum of the hydrogen and acceptor van der Waals distances.

<sup>3,12,13</sup> Multiple angular criteria were implemented in addition to distance to determine hydrogen bond formation. Elevation angle, or the angle formed between the methyl hydrogen and the plane of an sp<sup>2</sup> oxygen [Fig. 1(A)] was required to be < 50°, and the XH $\cdots$ Y angle was required to fall between 140 and 220°, where X and Y was either C or O. Angular criteria used to determine CH $\cdots$ C and OH $\cdots$ C were identical to those used for methyl CH $\cdots$ O hydrogen bonds. Additionally, a third X $\cdots$ H-O (where X is either C or O) angle that ranged from 150 to 220° was employed for sp<sup>3</sup> oxygen acceptors to rule out steric collisions with hydroxyl hydrogen atoms. Distance and angular distributions were volume-corrected by multiplying the counts by 1/*r*<sup>3</sup> and 1/sin $\theta$ , respectively.<sup>14–16</sup>

### Molecular dynamics (MD) simulation protocol

2XQZ was downloaded from the Protein Databank<sup>17</sup> and minimized for 50 steps of steepest decent minimization with heavy atom harmonic constraints. The structure was then solvated in 75.4 Å cubic volume of TIP3 water<sup>18</sup> and again minimized for 50 steps. Four equilibrium dynamic simulations were run consecutively with 1000 steps each at 100°, 200°, 250°, and 300° to slowly equilibrate the system. A production run using the CHARMM27 force field<sup>19</sup> was then performed for the system for 4.6 ns, using a 2-fs time step with SHAKE<sup>20</sup> to constrain the bond length of X-H bonds. SHAKE allows for 2-fs time steps and is common in hydrogen bond studies utilizing MD.<sup>21–23</sup> Nonbonded interactions were treated with a CUTNB of 12, CTOFNB of 9, CTONNB of 8 with both SHIFT and VSHIFT. A constant dielectric function was utilized for electrostatics with a dielectric constant of 1. Temperature was kept constant using a Nose-Hoover Thermostat,<sup>24</sup> and periodic boundary conditions were managed by the particle mesh Ewald method.<sup>25</sup> Coordinates were saved every 2 ps resulting in a total of 2328 frames. Both the minimization and simulation were setup using the MMTSB toolset.<sup>26</sup> A detailed list of commands can be found in the Supporting Information.

Methods describing QM calculations and the OMEGA program for analyzing hydrogen bond distances and angles are presented in the Supporting Information.

## RESULTS AND DISCUSSION

To evaluate the level of methyl CH $\cdots$ O hydrogen bonding in proteins with greater accuracy, we performed a survey of high-resolution neutron structures<sup>13</sup> in the PDB, guided by a recent evaluation of the accuracy of neutron crystal structures in determining hydrogen positions in proteins.<sup>10</sup> To systematically analyze methyl hydrogen bonding in these neutron structures, a new, flexible tool

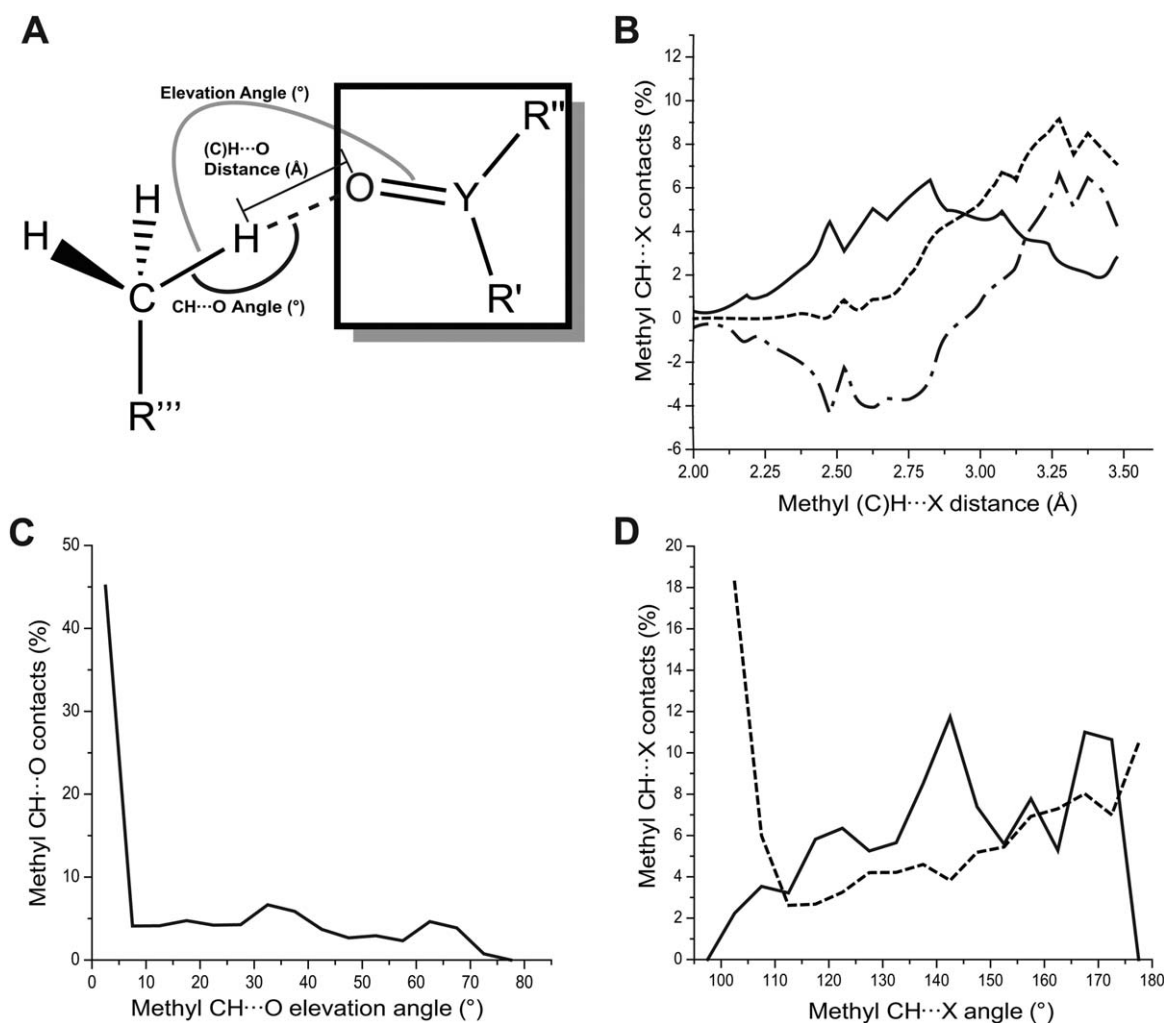


**Figure 1**

Survey of methyl CH...O hydrogen bonds in protein neutron structures. **A:** Depiction of angles and distances measured. **B:** Methyl hydrogen donor to acceptor distances in which the acceptor is oxygen (solid line) or carbon (dashed line). Dashed-dot line is the difference of the latter curves. **C:** Elevation angles of methyl CH...O hydrogen bonds. **D:** Methyl C—H...X angles in which X is oxygen (solid line) or carbon (dashed line).

was required to quickly analyze many different angular and distance parameters. Even the most flexible currently available hydrogen bonding programs<sup>27–33</sup> have limited customizability, both in terms of atoms and molecules that are allowed to be considered hydrogen bond donors and acceptors, as well as distances and angles that are allowed to be defined by the user to find interactions. To address this problem, we developed Open-ended Molecular fragments-based hydroGen bond Analyzer (OMEGA) (<https://github.com/jyesselm/omega>), a fully customizable hydrogen bonding detection and analysis toolkit that permits users to assign hydrogen bond donors and acceptors by chemical connectivity. In addition, an unlimited number of customizable distance, angle, and plane angle cut-offs can be specified to define whether an interaction meets the user's criteria of a hydrogen bond. Allowing for abstraction of hydrogen bonding constraints permits using

the same procedure on nonhydrogen bonding pairs as control data sets, or to analyze other forms of molecular contacts.

To evaluate whether an interaction qualifies as a hydrogen bond, we used an empirical definition, in which interactions are classified as hydrogen bonds if the atoms involved encroach within the combined van der Waals distances, and would otherwise be considered a steric clash.<sup>3,12</sup> Then, as hydrogen bonds typically display an angular dependence, the interaction angles are examined to reveal whether a hydrogen bond-like angular trend is observed, similar to previous studies examining CH...O hydrogen bonds<sup>3,7,12</sup> (Supporting Information).

We analyzed methyl CH...O hydrogen bonding in all neutron structures in which methyl hydrogen atoms are discernible,<sup>10</sup> to directly evaluate the level of CH...O hydrogen bonding in proteins. Unexpectedly, 36% of all

methyl CH $\cdots$ O contacts in proteins fell within the angular and distance criteria of being hydrogen bonds [Fig. 1(B)]. For comparison, the analogous percentage of all CH $\cdots$ O bonds in proteins, consisting primarily of C $\alpha$  backbone CH $\cdots$ O bonds in  $\beta$ -sheets, was reported by Derewenda *et al.* to be 13%, substantially less than that of the methyl groups observed here.<sup>12</sup> This juxtaposition is surprising for multiple reasons: (1) Unlike methyl groups, backbone CH $\cdots$ O hydrogen bonds are predisposed to form by secondary structure. (2) Methyl groups typically form weaker CH $\cdots$ O hydrogen bonds than the C $\alpha$  atom that is polarized through its covalent bonds to amide and carbonyl groups in the polypeptide chain. (3) Most methyl groups are thought to reside in the hydrophobic core of the protein, sequestered from hydrophilic oxygen atoms. By comparing the distribution of CH $\cdots$ O contacts to CH $\cdots$ C van der Waals contacts as a control, the CH $\cdots$ O distribution clearly favors interactions shorter than the van der Waals contact distance, similar to other CH $\cdots$ O hydrogen bonds.<sup>12</sup> Importantly, the angular distribution of the CH $\cdots$ O interactions is also consistent with hydrogen bond formation. The CH $\cdots$ O elevation angle displays a strong trend toward coplanarity [Fig. 1(C)]. Similarly, the C—H $\cdots$ O angle distribution displays a greater tendency toward linearity than that of C—H $\cdots$ C angles [Fig. 1(D)]. Combined with the distance distribution shown, the angular distributions clearly demonstrate that methyl groups in proteins form CH $\cdots$ O hydrogen bonds.<sup>6</sup>

Although the neutron structure analysis provides powerful information on the prevalence of methyl CH $\cdots$ O hydrogen bonds, they do not indicate whether these interactions are maintained through natural protein dynamics in solution, nor whether they are energetically stabilizing. To investigate this possibility, we chose one representative neutron structure, a perdeuterated R274N R276N mutant of  $\beta$ -lactamase (PDB accession code 2XQZ), for QM energy calculations and a short MD simulation to evaluate fluctuations in the CH $\cdots$ O hydrogen bonding side chains while retaining the overall protein conformation. This structure contains a total of 171 methyl groups, 27 of which form CH $\cdots$ O hydrogen bonds in the neutron structure. In total, 46% of all methyl CH $\cdots$ O contacts in this structure that satisfy the angular criteria for hydrogen bond formation also fall within the distance criteria of being a hydrogen bond.

To evaluate whether these methyl CH $\cdots$ O hydrogen bonds are energetically stabilizing in the conformations found within the protein, we extracted methyl CH $\cdots$ O hydrogen bond pairs for QM energy calculations. Before calculating the energy of the pairs, each was examined for contacts other than methyl CH $\cdots$ O hydrogen bonds that could contribute to the interaction energy. After removing those that had other interactions, 12 hydrogen bonding pairs remained, and the energies of these isolated interactions were calculated without geometry opti-

mization. Thus, the energies presented here (Table I) are likely correlated with the hydrogen bonding energy of the pairs within the crystal structure, as opposed to an optimized arrangement. Notably, the average interaction energy of  $-0.6$  kcal/mol using MP2 and  $-2.4$  kcal/mol using the density functional with dispersion (DFT-D; wB97xD) across the hydrogen bonds indicates that these interactions are on average slightly stabilizing. Notably, the DFT-D method resulted in uniformly more stabilizing interactions than those calculated by MP2, likely due to their different handling of dispersive forces. Alanine methyl groups formed the strongest hydrogen bonds, with energies ranging from  $-1.0$  to  $-4.4$  kcal/mol, most likely due to the electron withdrawing properties of the neighboring backbone carbonyl and amide groups, and consistent with weak to intermediate strength CH $\cdots$ O hydrogen bonds.<sup>4,5</sup> Threonines also uniformly formed stabilizing interactions, whereas for leucines and isoleucines, the interactions were only slightly stabilizing, or in some cases, predicted to be slightly destabilizing by MP2. This observation was not surprising, given the multiple bond separation between the isoleucine and leucine methyl groups and the electron withdrawing backbone. Given the overall weak nature of the interactions, and that they are not universally stabilizing within the crystal by both QM calculation methods, it was unclear whether methyl CH $\cdots$ O hydrogen bonds are important enough to be maintained in the process of protein dynamics.

To examine whether these methyl CH $\cdots$ O hydrogen bonds exist in a dynamic, fluctuating protein, we performed a 4.6 ns MD simulation of the test protein. The short time of the simulation was chosen to keep the protein backbone conformation in a similar position to that found in the neutron structure, but allow significant side-chain motion. Examining the CH $\cdots$ O hydrogen bonds that were found within the neutron structure revealed that they are maintained to a much greater degree than those that are formed within the MD simulation but are not present in the neutron structure [Fig. 2(A)]. This observation suggests that the CH $\cdots$ O hydrogen bonding patterns observed in the neutron structures are maintained in solution.

To address whether the pairs of methyl-oxygen CH $\cdots$ O hydrogen bonds participate in correlated motion in the MD simulation, as would be expected of hydrogen bonds, we used a simplified metric to evaluate hydrogen bonding based on dihedral angles [Fig. 2(B)]. In this metric, the dihedral angle about the C<sub>methyl</sub>-R bond is measured using two alternative fourth atoms: the methyl hydrogen, or the oxygen acceptor. In the case that the two dihedral angles are the same, the C<sub>methyl</sub>-H bond vector resides within the same plane as the C<sub>methyl</sub> $\cdots$ O vector. As such, subtracting these two dihedral angles provides a metric for the angular overlap of the C<sub>methyl</sub> $\cdots$ O and C<sub>methyl</sub>-H bond vector. A representative distribution of these dihedrals for a CH $\cdots$ O hydrogen

bond pair from the MD simulation is shown in Figure 2(B). As expected, the multiple hydrogen peaks represent the different methyl hydrogen energy wells sampled throughout the simulation, whereas the oxygen atoms more frequently only displayed one peak, representing a single energy well that results in a relatively stationary oxygen atom.

To quantify the overlap of the hydrogen and oxygen atoms of CH...O hydrogen bonding pairs in the simulation, we fit the hydrogen and oxygen peaks using Gaussian functions, and analyzed both the standard deviations and mean positions of the peaks to evaluate whether the CH...O hydrogen bonding pairs exhibited correlated position and motion within the MD simulation. Plotting the difference in standard deviations of the dihedral angles ( $y$  axis) versus the normalized difference between the mean values of the oxygen and hydrogen dihedral angles ( $x$  axis) yields a distribution that encapsulates both the breadth of motion, as well as the degree of angular overlap of the hydrogen bonding pair [Fig. 2(C)] Other less frequent variations that were observed are shown in aggregate in Supporting Information Figure S1. The coloring of the  $z$  axis for this distribution represents the total number of frames that the CH...O hydrogen bond was observed to exist in the pair during the MD simulation. The distribution of the methyl groups and oxygen atoms forming CH...O hydrogen bonds appears substantially different than that of a random distribution, suggesting that donor and acceptor atoms in the CH...O hydrogen bonding pairs influence each other's respective positions. Further, these pairs tend to exhibit relatively small differences in both their dihedral angle standard deviations and mean values compared to the random atoms pairs, implying that the CH...O hydrogen bonding pairs experience correlated motion during the MD simulation. To quantify the difference in the hydrogen bonding versus random distributions, we analyzed them using the Jensen-Shannon Divergence (JSD) metric, which uses a scale of 0 to 1 to evaluate dis-similarity in distributions. The JSD has been a critical tool in assessing the similarity of two given distributions and is utilized in a wide diversity of studies including structural biology and bioinformatics.<sup>34–36</sup> The JSD analysis demonstrates that as the distributions are analyzed as a function of increasing number of frames in the MD simulation in which the CH...O hydrogen bond is observed [i.e., increasing  $z$  axis values in Fig. 2(C)], the hydrogen bonding and random distributions diverge significantly [Fig. 2(D)]. As a control, we also used random cutoffs in place of the minimum CH...O hydrogen bond count. By comparing these two methods of generating cutoffs, we found that while the distributions are nearly identical when the total frame cutoff for observing a CH...O hydrogen bond is small, they become increasingly different as the number of frames in which a hydrogen bond is observed increases in the MD simula-

**Table 1**

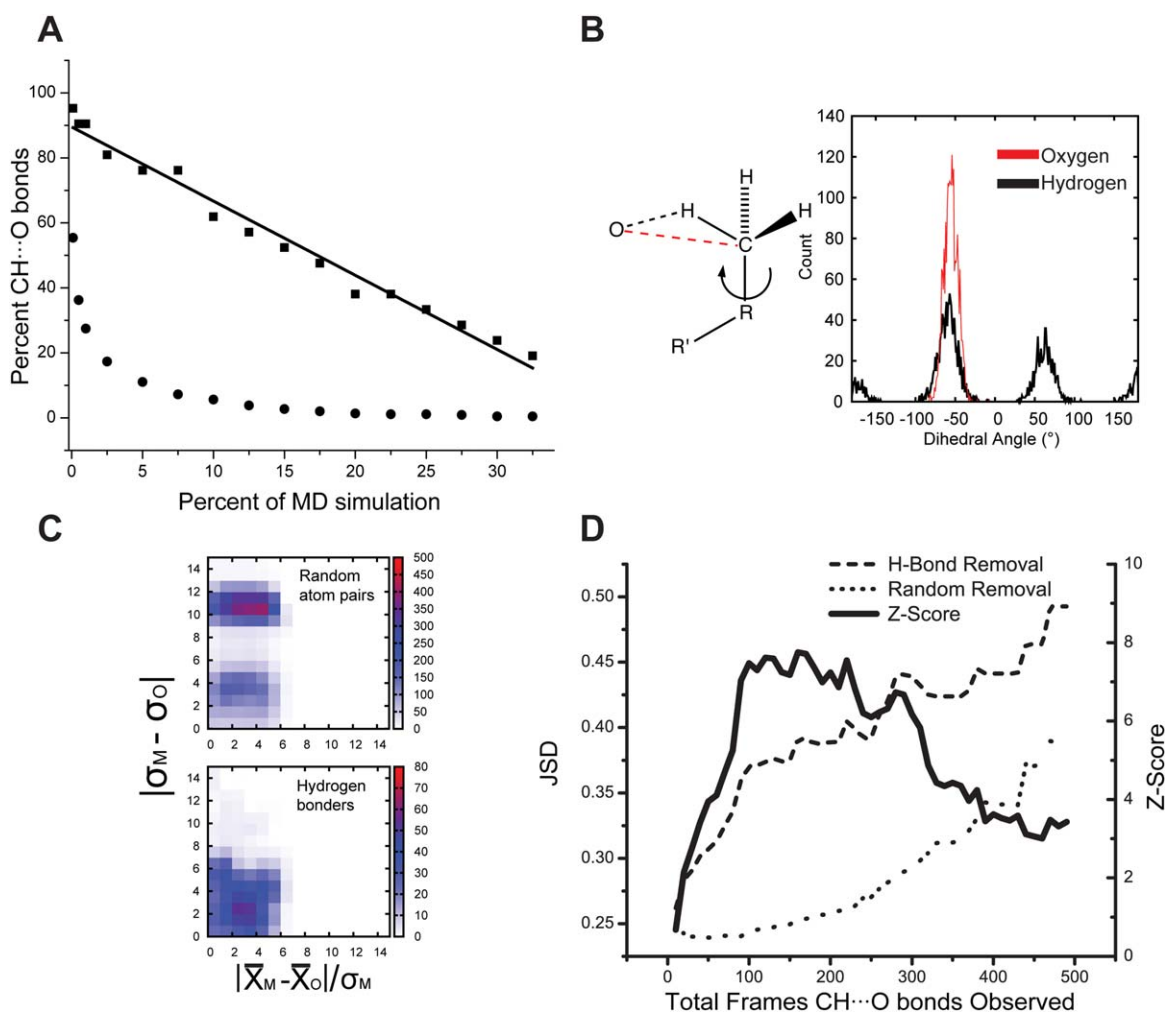
Counterpoise Interaction Energies of Methyl CH...O hydrogen bonds in  $\beta$ -lactamase R274N R276N mutant

	Donor				Acceptor		wB97 $\times$ D Energy (kcal/mol)	MP2 Energy (kcal/mol)
CB	ALA	250	0	ALA	191		-4.4	-2.9
CB	ALA	34	0	VAL	19		-3.3	-2.4
CB	ALA	106	0	LEU	94		-3.8	-1.0
CG2	ILE	69	0	ALA	81		-1.6	0.3
CD1	LEU	171	0	LEU	165		-2.2	-0.3
CD2	LEU	171	0	ALA	50		-1.3	-0.2
CD1	LEU	31	OE1	GLN	29		-1.6	0.4
CD1	LEU	53	0	GLN	175		-3.0	1.0
CG2	THR	188	0	GLN	100		-2.8	-1.8
CG2	THR	207	OG1	THR	188		-1.9	-0.4
CG2	THR	187	0	GLY	185		-1.3	-0.3
CG2	THR	152	0	ASP	148		-1.4	-0.1

tion [Fig. 2(D)]. Together, these trends clearly demonstrate that the methyl-oxygen CH...O hydrogen bonding groups in the simulation that are formed for greater amounts of time in the MD simulation have greater angular overlap and correlated motion compared with those which are formed transiently.

Together, the results presented here demonstrate that CH...O hydrogen bonding occurs at remarkably high rate for methyl group donors, the carbon atoms with the lowest hydrogen bond potential in proteins. Computational analysis suggests that although these interactions are weak, they are maintained through protein dynamics and participate in correlated motion. It is intriguing to consider these results in the context of the well-accepted hydrophobic collapse model of protein folding. In this model, the water forms semi-rigid cages surrounding hydrophobic regions of the protein in its unfolded state, reducing the solvent entropy. By sequestering the hydrophobic regions away from the water, the cages are released and the water entropy increases. Notably, the calculations performed here suggest that the energy of protein methyl CH...O hydrogen bonds are weaker than the hydrogen bonds of water-water dimers ( $\sim -5$  kcal/mol),<sup>4</sup> suggesting that although these methyl groups are capable of forming CH...O hydrogen bonds, they are not able to effectively compete with the water-water hydrogen bonds of the hydrophobic cages. However, within the protein core, these methyl groups are free to participate in hydrogen bonding without affecting the solvent entropy.

These observations imply that side chain methyl CH...O hydrogen bonds may play a role in the stabilization of buried oxygens in the hydrophobic core of proteins, similar to the function of the C $\alpha$  positions in  $\beta$ -sheets.<sup>2,37</sup> QM studies have previously suggested that CH...O hydrogen bonds could contribute to protein folding due to a relatively small desolvation penalty associated with forming the hydrogen bond in the protein interior, as opposed to with water,<sup>38</sup> and it could be that the methyl group CH...O hydrogen bonds aid in protein folding by this mechanism.

**Figure 2**

Analysis of methyl CH...O hydrogen bonds in  $\beta$ -lactamase R274N R276N mutant MD simulation. **A:** Methyl CH...O hydrogen bonds observed in neutron structure (squares) are formed more often than those not observed in neutron structure (circles), quantified using multiple angles and distance cutoffs as used in the neutron structure analysis. (See Supporting Information). **B:** Dihedral angles used in overlap calculations and representative trace of hydrogen bonding pair in which the fourth atom is an oxygen acceptor (red) or methyl hydrogen donor (black) atom. **C:** Aggregate of dihedral angle overlap traces (example overlap trace shown in panel B). X and Y axes depict the differences between the normalized mean position of the dihedral angles, and standard deviations of the hydrogen bonding pair, respectively. Z-axis shows the number of MD frames. **D:** Quantification of dihedral angle overlap depicted in panel C. Threshold cutoffs determined using frames of hydrogen bond formation (dashed line) or randomly (dotted line). Statistical significance between these two lines depicted by Z-score (solid line).

Small desolvation penalties have been critical to modeling protein folding using coarse-grained approaches. Karanicolas and Brooks<sup>39</sup> found that modifying the Lennard-Jones potential yielded a small energy barrier that represented the desolvation penalty of forming a favorable contact. Following a different strategy, Cheung *et al.*<sup>40</sup> included a separate desolvation term that came into effect at near-ideal contact geometry. These and more recent modifications<sup>41</sup> to the classical molecular mechanics force field increased agreement with experimental protein folding data by better modeling the process of packing interior side chains during folding, finding that an attractive interaction between hydrophobic side chains and water alters the cooperativity of pro-

tein folding. Likely, the attractive interaction identified in these studies is in fact the methyl hydrogen bonding presented here.

Garcia-Moreno and coworkers previously demonstrated that the hydrophobic core of Staphylococcal nuclease is resistant to mutations of glutamic and aspartic acid in 26 individual positions with only minor local rearrangement.<sup>42,43</sup> These mutated residues have extreme shifts in pKa and their side chains must be satisfied by a hydrogen bond network to stably exist within the protein. Although the previous interpretation of these mutations is that water channels are used to satisfy these charged residues, it is also plausible that CH...O hydrogen bonds assist in the stabilization of these charges. Given the high propensity of

methyl groups to reside in the interior of the protein, it is conceivable that charged and/or polar residues are in large part accommodated in proteins by forming CH...O hydrogen bonds with side chains. Further studies are needed to explore to what extent these hydrogen bonds contribute protein stabilization and folding.

## ACKNOWLEDGMENTS

The authors wish to thank Samuel Krimm, Noemi Mirkin, and Steve Scheiner for reading the manuscript and providing insightful comments, and James Bardwell for use of his computational cluster allocation.

## REFERENCES

- Desiraju GR, Steiner T. The weak hydrogen bond. Oxford: Oxford University Press; 1999.
- Horowitz S, Trievel RC. Carbon-oxygen hydrogen bonding in biological structure and function. *J Biol Chem* 2012;287:41576–41582.
- Horowitz S, Dirk LM, Yesselman JD, Nimtz JS, Adhikari U, Mehl RA, Scheiner S, Houtz RL, Al-Hashimi HM, Trievel RC. Conservation and functional importance of carbon-oxygen hydrogen bonding in AdoMet-dependent methyltransferases. *J Am Chem Soc* 2013;135:15536–15548.
- Gu YL, Kar T, Scheiner S. Fundamental properties of the CH center dot center dot center dot O interaction: is it a true hydrogen bond? *J Am Chem Soc* 1999;121:9411–9422.
- Kryachko ES, Zeegers-Huyskens T. Theoretical study of the CH center dot center dot center dot O interaction in fluoromethanes center dot H<sub>2</sub>O and chloromethanes center dot H<sub>2</sub>O complexes. *J Phys Chem A* 2001;105:7118–7125.
- Steiner T, Desiraju GR. Distinction between the weak hydrogen bond and the van der Waals interaction. *Chem Commun* 1998: 891–892.
- Steiner T. Influence of C-H center dot center dot center dot O interactions on the conformation of methyl groups quantified from neutron diffraction data. *J Phys Chem A* 2000;104:433–435.
- Panigrahi SK, Desiraju GR. Strong and weak hydrogen bonds in the protein-ligand interface. *Proteins* 2007;67:128–141.
- Sarkhel S, Desiraju GR. N - H.O, O - H.O, and C - H.O hydrogen bonds in protein-ligand complexes: strong and weak interactions in molecular recognition. *Proteins: Struct Funct Genet* 2004;54: 247–259.
- Chen JC, Hanson BL, Fisher SZ, Langan P, Kovalevsky AY. Direct observation of hydrogen atom dynamics and interactions by ultra-high resolution neutron protein crystallography. *Proc Natl Acad Sci USA* 2012;109:15301–15306.
- Arunan E, Desiraju GR, Klein RA, Sadlej J, Scheiner S, Alkorta I, Clary DC, Crabtree RH, Dannenberg JJ, Hobza P, Kjaergaard HG, Legon AC, Mennucci B, Nesbitt DJ. Definition of the hydrogen bond (IUPAC Recommendations 2011). *Pure Appl Chem* 2011;83: 1637–1641.
- Derewenda ZS, Lee L, Derewenda U. The occurrence of C-H-center-dot-center-dot-center-dot-O hydrogen-bonds in proteins. *J Mol Biol* 1995;252:248–262.
- Taylor R, Kennard O. Crystallographic evidence for the existence of C-H.O, C-H.N, and C-H.C1 hydrogen-bonds. *J Am Chem Soc* 1982;104:5063–5070.
- Balasubramanian R, Chidambaram R, Ramachandran Gn. Potential functions for hydrogen bond interactions II. Formulation of an empirical potential function. *Biochim Biophys Acta* 1970;221: 196–206.
- Pierce AC, Sandretto KL, Bemis GW. Kinase inhibitors and the case for CH center dot center dot center dot O hydrogen bonds in protein-ligand binding. *Proteins: Struct Funct Genet* 2002;49:567–576.
- Kroon J, Kanters JA. Nonlinearity of Hydrogen-Bonds in Molecular-Crystals. *Nature* 1974;248(5450):667–669.
- Tomanicek SJ, Wang KK, Weiss KL, Blakeley MP, Cooper J, Chen Y, Coates L. The active site protonation states of perdeuterated Toho-1 beta-lactamase determined by neutron diffraction support a role for Glu166 as the general base in acylation. *FEBS Lett* 2011;585: 364–368.
- Jorgensen WL, Chandrasekhar J, Madura JD, Impey RW, Klein ML. Comparison of simple potential functions for simulating liquid water. *J Chem Phys* 1983;79:926–935.
- Brooks BR, Brooks CL, Mackerell AD, Nilsson L, Petrella RJ, Roux B, Won Y, Archontis G, Bartels C, Boresch S, Caflisch A, Caves L, Cui Q, Dinner AR, Feig M, Fischer S, Gao J, Hodoseck M, Im W, Kuczera K, Lazaridis T, Ma J, Ovchinnikov V, Paci E, Pastor RW, Post CB, Pu JZ, Schaefer M, Tidor B, Venable RM, Woodcock HL, Wu X, Yang W, York DM, Karplus M. CHARMM: the biomolecular simulation program. *J Comput Chem* 2009;30:1545–1614.
- Ryckaert JP, Ciccotti G, Berendsen HJC. Numerical-integration of Cartesian equations of motion of a system with constraints - molecular-dynamics of N-alkanes. *J Comput Phys* 1977;23:327–341.
- Auffinger P, Louise-May S, Westhof E. Molecular dynamics simulations of solvated yeast tRNA(Asp). *Biophys J* 1999;76:50–64.
- Fleming PJ, Rose GD. Do all backbone polar groups in proteins form hydrogen bonds? *Protein Sci* 2005;14:1911–1917.
- Garcia AE, Sanbonmatsu KY. alpha-Helical stabilization by side chain shielding of backbone hydrogen bonds. *Proc Natl Acad Sci USA* 2002;99:2782–2787.
- Nose S, Klein ML. Constant pressure molecular-dynamics for molecular-systems. *Mol Phys* 1983;50:1055–1076.
- Essmann U, Perera L, Berkowitz ML, Darden T, Lee H, Pedersen LG. A smooth particle mesh Ewald method. *J Chem Phys* 1995;103: 8577–8593.
- Feig M, Karanicolas J, Brooks CL. MMTSB Tool Set: enhanced sampling and multiscale modeling methods for applications in structural biology. *J Mol Graph Model* 2004;22:377–395.
- Mcdonald IK, Thornton JM. Satisfying hydrogen-bonding potential in proteins. *J Mol Biol* 1994;238:777–793.
- Durrant JD, McCammon JA. HBonanza: a computer algorithm for molecular-dynamics-trajectory hydrogen-bond analysis. *J Mol Graph Model* 2011;31:5–9.
- Kumar P, Kailasam S, Chakraborty S, Bansal M. MolBridge: a program for identifying nonbonded interactions in small molecules and biomolecular structures. *J Appl Cryst* 2014;47:1772–1776.
- Lindauer K, Bendic C, Suhnel J. HBExplore - A new tool for identifying and analysing hydrogen bonding patterns in biological macromolecules. *Comput Appl Biosci* 1996;12:281–289.
- Babu MM. NCI: a server to identify non-canonical interactions in protein structures. *Nucleic Acids Res* 2003;31:3345–3348.
- Tiwari A, Panigrahi SK. HBAT: a complete package for analysing strong and weak hydrogen bonds in macromolecular crystal structures. *In Silico Biol* 2007;7:651–661.
- Tina KG, Bhadra R, Srinivasan N. PIC: protein interactions calculator. *Nucleic Acids Res* 2007;35(Web Server issue):W473–476.
- Yang S, Salmon L, Al-Hashimi HM. Measuring similarity between dynamic ensembles of biomolecules. *Nat Methods* 2014;11: 552–554.
- Capra JA, Singh M. Predicting functionally important residues from sequence conservation. *Bioinformatics* 2007;23:1875–1882.
- Ofran Y, Rost B. Analysing six types of protein-protein interfaces. *J Mol Biol* 2003;325:377–387.
- Scheiner S. Relative strengths of NH center dot center dot O and CH center dot center dot O hydrogen bonds between polypeptide chain segments. *J Phys Chem B* 2005;109:16132–16141.

38. Scheiner S, Kar T. Effect of solvent upon CH center dot center dot center dot O hydrogen bonds with implications for protein folding. *J Phys Chem B* 2005;109:3681–3689.
39. Karanicolas J, Brooks CL, III. The origins of asymmetry in the folding transition states of protein L and protein G. *Protein Sci* 2002; 11:2351–2361.
40. Cheung MS, Garcia AE, Onuchic JN. Protein folding mediated by solvation: water expulsion and formation of the hydrophobic core occur after the structural collapse. *Proc Natl Acad Sci USA* 2002;99: 685–690.
41. Chen T, Chan HS. Effects of desolvation barriers and sidechains on local-nonlocal coupling and chevron behaviors in coarse-grained models of protein folding. *Phys Chem Chem Phys* 2014;16:6460–6479.
42. Isom DG, Castaneda CA, Cannon BR, Velu PD, Garcia-Moreno EB. Charges in the hydrophobic interior of proteins. *Proc Natl Acad Sci USA* 2010;107:16096–16100.
43. Isom DG, Cannon BR, Castaneda CA, Robinson A, Garcia-Moreno B. High tolerance for ionizable residues in the hydrophobic interior of proteins. *Proc Natl Acad Sci USA* 2008;105:17784–17788.